Materials Horizons

Printing Dynamic Color Palettes and Layered Textures through Modeling-Guided Stacking of Electrochromic Polymers

Journal:	*Materials Horizons*
Manuscript ID	MH-COM-07-2021-001098.R1
Article Type:	Communication
Date Submitted by the Author:	04-Oct-2021

Complete List of Authors:	Chen, Ke; Purdue University, Chemistry Wu, Yukun; Purdue University, Chemistry You, Liyan; Purdue University, Chemistry Wu, Wenting; Purdue University, Chemistry Wang, Xiaokang; Purdue University Zhang, Di; Purdue University, School of Materials Engineering Elman, James; Filmetrics Application Lab, Ahmed, Mustafa; Purdue University, Chemistry Wang, Haiyan; Purdue University System, MSE; Neil Armstrong Engineering Building Zhao, Kejie; Purdue University Mei, Jianguo; Purdue University, Chemistry

COMMUNICATION

Printing Dynamic Color Palettes and Layered Textures through Modeling-Guided Stacking of Electrochromic Polymers

Received 00th January 20xx,
Accepted 00th January 20xx

DOI: 10.1039/x0xx00000x

Ke Chen[a], Yukun Wu[a], Liyan You[a], Wenting Wu[a], Xiaokang Wang[b], Di Zhang[c], James F. Elman[d], Mustafa Ahmed[a], Haiyan Wang[c], Kejie Zhao[b], Jianguo Mei [a,*]

In printable electrochromic polymer displays, a wide color gamut, precise patterning, as well as controllable color switching are important. Yet, it is a significant challenge to achieve such features synergistically. Here, we present a solution-processable ECP stacking scheme, where a crosslinker is co-processed with three primary ECPs (ECP-Cyan, ECP-Magenta, and ECP-Yellow), endows them with solvent-resistant properties, and allows them to be sequentially deposited. Via varying the film thickness of each ECP layer, a full-color palette can be constructed. The ECP stacking strategy is further integrated with photolithography. Delicate multilayer patterns with overhang and undercut textures can be generated, allowing for information display with spatial dimensionality. In addition, via modulating the stacking sequence, the electrochemical onset potentials of ECP components can be synchronized to reduce unwanted intermediate colors that are often found in co-processed ECPs. Should specific color properties be desired, COMSOL modeling could be applied to guide the stacking. We believe this ECP stacking strategy opens an avenue for electrochromic printing and display.

New concepts

Expanding the color palettes of electrochromic polymers (ECPs) is crucial for polymer electrochromics. Equally, construction of delicate patterns and controllable switching of color states are also prerequisites in electrochromic displays. Here, we report a solution-processable ECP stacking strategy, where a crosslinker is co-processed with three primary ECPs. Under ultraviolet light illumination, the cross-linking of the ECPs is triggered which endows them with solvent-resistant properties and allows them to be sequentially deposited. By varying the thickness of each stacked layer, a full-color gamut can be obtained. In addition, the stacking strategy is compatible with photolithography printing technique, which enables the construction of ultraprecise ECP patterns with delicate overhang and undercut layered textures. This opens an avenue for versatile ECP color printing and display. Furthermore, via modifying the stacking sequence, the electrochemical onset potentials of ECP components can be synchronized to reduce unwanted intermediate colors that are often seen in co-processed polymers. Last, COMSOL modeling is used to forecast the spectroscopic characteristics and color appearance of the multilayer ECPs, which provides theoretical guidance on ECP design and stacking.

Introduction

Electrochromic polymer (ECP) changes its color due to electrochemical redox reactions, known as electrochromism. Polymer electrochromics can be fast, cyclically stable, and energy-efficient, making them hold enormous potential in the applications of displays,[1–4] optical shutters (smart window, sunglass),[5–7] and electronic papers.[8] To pursue future printable electrochromic displays, a wide color range, controllable color switching, as well as precise on-demand patterns, among others, are essential elements to explore. At present, a full-color palette of ECPs has been achieved via tuning molecular structures in synthesis or mixing ECPs with primary colors based on color mixing theory.[9–11] In the synthetic approach, varying the backbones or sidechains of electrochromic polymers to achieve a fine color control is complicated and time-consuming, due to the sophisticated polymer structures and color relationships.[10] In contrast, color mixing is a well-established strategy to obtain desired colors and it has been implemented by ECP blending or stacking.[12,13] In polymer blending, polymer solutions are blended first and deposited on substrates. For example, Reynolds et al., reported a fine color tuning through

[a] Department of Chemistry, Purdue University, West Lafayette, IN 47907, United States
[b] School of Mechanical Engineering, Purdue University, West Lafayette, IN, 47907, United States
[c] School of Materials Engineering, Purdue University, West Lafayette, IN 47907, United States
[d] Filmetrics, Inc., A KLA company, 250 Packett's Landing Fairport, NY 14450, United States

Electronic Supplementary Information (ESI) available: [details of any supplementary information available should be included here]. See DOI: 10.1039/x0xx00000x

blending cyan, magenta, yellow ECPs.[14] In spite of simplicity and accessibility, the blending approach has its limitations in terms of color control. Due to the disparity of electrochemical onset potentials between the blended ECPs, polymers with lower onset will get oxidized first under a constant potential, inducing unwanted intermediated colors. Alternatively, stacking ECPs is a promising way to facilitate the color mixing, where polymers with primary colors are sequentially deposited to generate secondary or more sophisticated color shades. Furthermore, the order of polymers being electrochemically doped can be adjusted through the polymer deposition sequence, which can minimize intermediate colors. Additionally, layered textures and patterns can be constructed based on polymer stacking. Since humans have both tactile and visual texture perception, the stacked patterns will be able to convey more information.[15,16] To our knowledge, the stacking strategy has mostly been demonstrated through in-situ electropolymerization of multilayer ECPs on electrodes, which is often incompatible with site-specific large-scale patterning.[17] In this work, we present a stacking scheme for solution-processable ECPs with the integration of photolithography and printing to realize full colors and layered textures, laying a foundation for future electrochromic display. Further, we demonstrate that the electrochemical onset potentials of stacked ECPs can be synchronized to reduce intermediate colors via modulating the stacking sequence. Finally, we use finite element analysis (FEA) to guide the design and stacking of ECPs to achieve desired colors. The modeling framework allows for numerical prediction of the spectroscopic characteristics and color appearance of ECPs.

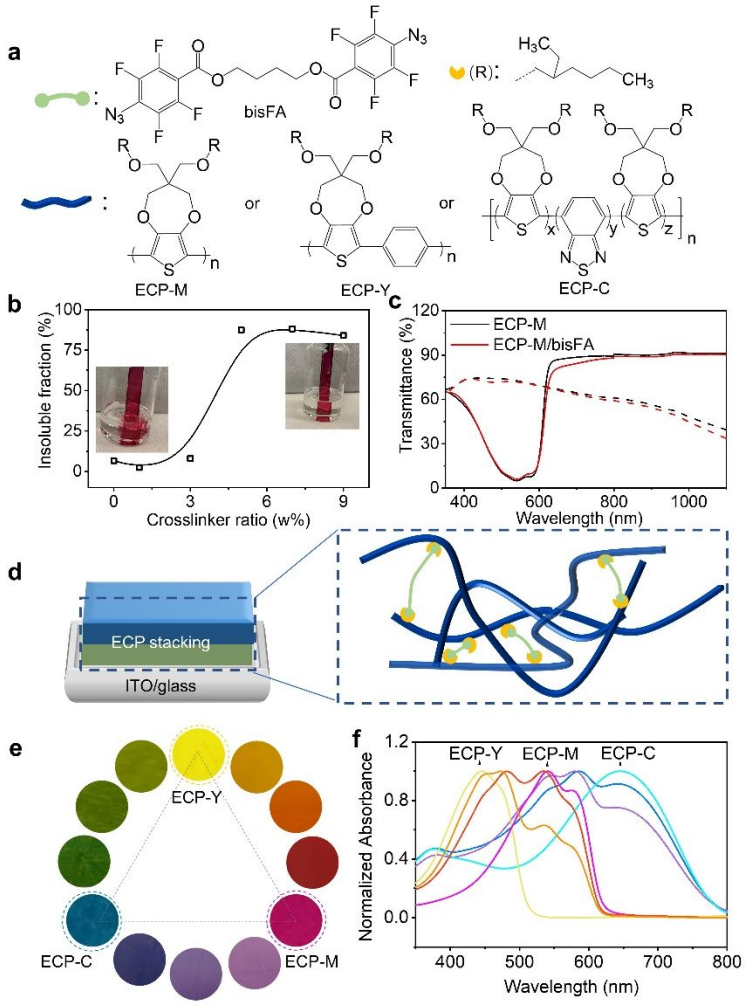

Fig. 1 Building color palettes via stacking cross-linked electrochromic polymers. (a) Molecular structures of crosslinker (bisFA) and three primary electrochromic polymers (ECP-M, ECP-Y, and ECP-C). R shows the side chain structures of the ECPs. x-, y-, and z-values represent the equivalents of corresponding monomers during synthesis. (b) Insoluble fraction as a function of crosslinker weight ratio to ECP-M. The inset pictures show the pure and crosslinked ECP-M films in chloroform solutions. (c) Spectroelectrochemistry of pure ECP-M and cross-linked ECP-M. (d) Schema of a double-layer ECP stacking. The zoom-in view shows detailed cross-linked ECP, where the crosslinker connects the sidechains of ECPs. (e) Pictures and (f) absorbance spectra of a full-color palette prepared by stacking two of the three primary ECPs with a variety of thicknesses.

To implement the stacking, each polymer layer needs to be solvent-resistant and avoid the dissolution during the subsequent coatings. In our study, a well-studied bis(fluorophenyl azide) (bisFA) crosslinker, whose structure is shown in **Figure 1a**, is chosen to co-process with ECPs to introduce the solvent resistance.[18] The structure of the crosslinker is confirmed by NMR in **Figure S1**. Following the CMY subtractive color mixing model, three primary ECPs from the poly((3,4-propylenedioxy-thiophene) (PProDOT) family are employed for stacking, which are magenta, yellow and cyan, respectively in neutral states.[19–23] These polymers are denoted as ECP-M, ECP-Y, and ECP-C, as shown in **Figure 1a**. Their structures are confirmed by NMR in **Figure S2**. Their molecular weight and dispersity information are characterized by gel permeation chromatography (GPC) as shown in **Figure S3** and are summarized in **Table S1**. To examine the photo-cross-linking behaviors of the electrochromic polymer (ECPs)/crosslinker, we first use poly(3,4-propylenedioxythiophene) (ECP-M) as the study model. The crosslinker (bisFA) is co-processed with ECP-M with bisFA/ECP-M weight ratio from 0 % to 9 %, and they are exposed to ultraviolet (UV) light in a nitrogen-filled glovebox for 5 minutes to complete the cross-linking. During the UV exposure, the predominant cross-linking reaction is the nitrene insertion into the alky chain of the polymers.[24,25] This photo-cross-linking process is confirmed by Fourier-transform infrared spectroscopy in **Figure S4**, where a loss of N_3 peak (ν_{as}=2125 cm^{-1}; ν_a=1255 cm^{-1}) and formation of characteristics C-N (ν_{as} $\approx$ 1216) and N-H (ν $\approx$ 3360) bonds are observed after the UV exposure. Differential scanning calorimetry (DSC) data in **Figure S5** show that crosslinked ECP-M exhibits higher Tc temperature compared with pure ECP-M. This may be due to a more fixed molecular structure caused by side chain connections. To quantify the cross-linking efficiency, the cross-linked films are immersed in the chloroform for 5 minutes followed by a further chloroform washing. The insoluble fractions of the films are defined as the quotient between their absorbance after solvent washing and their initial absorbance at 540 nm (the maximum absorption of ECP-M). As plotted in **Figure 1b**, with the addition of 5 w% to 9 w% of crosslinker, the electrochromic film exhibits more than 85% of insoluble fraction. The absorbance spectra of the ECPs with different amounts of crosslinkers are also examined to study the possible influence of the cross-linking on the molecular packing of the ECP-M. As shown in **Figure S6**, a higher crosslinker-to-ECP weight ratio leads to a lower 0-0 to 0-1 vibronic peak ratio of the ECP-M, indicating a weaker ECP intrachain ordering. Considering the cross-linking efficiency, 5 w% of crosslinker is selected to further study the impact of the cross-linking on the electrochemical and electrochromic performance of the ECP-M. This investigation is performed in a three-electrode cell with Ag/AgCl as a reference electrode, Pt wire as a counter electrode, and 0.2 M LiTFSI (Lithium bis(trifluoromethanesulfonyl)imide)/ PC (propyl carbonate) as supportive electrolyte. As shown in **Figure 1c**, compared with pure ECP-M, the cross-linked one exhibits almost identical transmittance in both colored (reduced) and bleached (oxidized) states, suggesting a minimum impact of the cross-linking on their electrochromic performances. The switching kinetics and cyclic voltammograms of the pure and cross-linked ECP-M are also compared in **Figure S7**, which presents a negligible difference. Under the same cross-linking conditions, the other two primary ECPs (ECP-C and ECP-Y) also exhibit high insoluble fractions (both are 98%) and unaffected electrochromic performances, as illustrated in **Figure S8** and **S9**. With a cross-linked ECP, another layer of ECP can be spin-coated on its top, forming a double-layer electrochromic thin film, as demonstrated in a scanning electronic microscopic image in **Figure S10**. As a result, by stacking two of the three primary electrochromic polymers with a variety of thicknesses, a color palette with hues covering the whole visible spectrum can be obtained. A schematic illustration of electrochromic stacking and cross-linking are illustrated in **Figure 1d**. The pictures and UV-Vis spectra of the color palette are shown in **Figure 1e** and **Figure 1f**, respectively. The raw transmittance spectra and thickness information for each color in the palette have been summarized in **Figure S11** and **Table S2**.

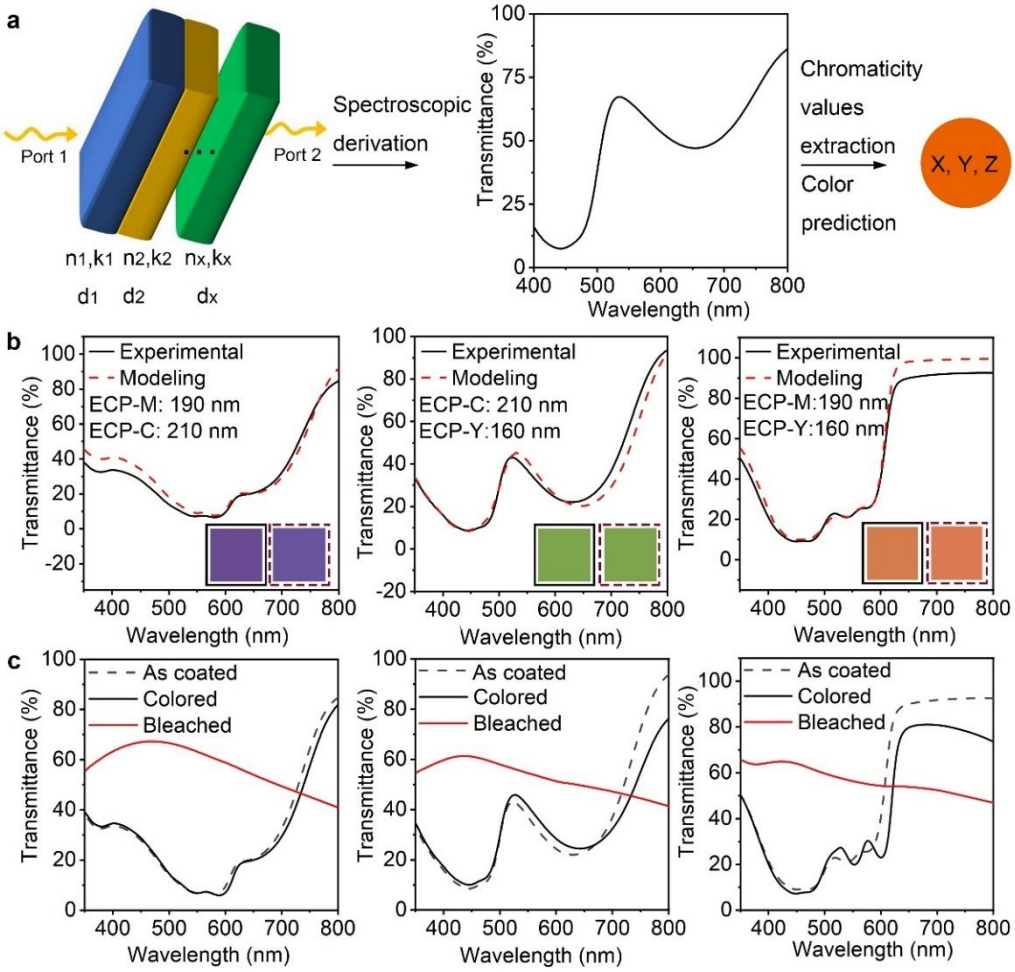

Fig. 2 Optical modeling-guided double-layer ECP stackings. (a) Workflow of the optical modeling. (b) Experimental vs. modeling spectra of the double-layer ECPs consisting of various polymer thicknesses. The colors in the solid and dashed boxes are predicted by experimental and modeling spectra, respectively. (c) Spectroelectrochemistries of the double-layer ECPs.

After demonstrating the feasibility of multilayer ECP deposition, we conduct finite elemental analysis (FEA) to simulate the electromagnetic field-ECP stacking interactions using COMSOL, whereby the spectroscopic characteristics and color appearances of the ECP stackings can be theoretically predicted. The workflow of the optical modeling is shown in **Figure 2a**. A multilayer geometry with a high width-to-thickness ratio is built to simulate the stacked polymer thin films. Depolarized electromagnetic waves (port 1 and port 2) with the wavelength from 400 to 800 nm are applied perpendicularly to the geometry from top to the bottom. Intrinsic values of each polymer—refractive index (n), extinction coefficient (k), and thickness (d)—are applied respectively to each layer of the model to study the interaction between electromagnetic waves and the polymer stacking system. The transmittance or reflectance spectra can be derived as the simulated results. The chromaticity values are extracted from the spectra to predict the color appearance of the system. The detailed simulation process is included in **Supplementary Notes**.

We first implement the optical modeling to double-layer ECPs. To this end, two-layer geometries are constructed and two out of the three primary ECPs (ECP-C, ECP-M, ECP-Y) are assigned to the geometry, generating three stacking scenarios, as shown in **Figure 2b**. The refractive indices and absorption coefficients of the three polymers are measured by Filmetrics and shown in **Figure S12**. In all three stacking scenarios, the thicknesses of ECP-C, ECP-M and ECP-Y are set to 210 nm, 190 nm, and 160 nm, respectively. As the computational results, the transmittance of the three double-layer ECPs is calculated and shown with red dashed curves. Next, we perform experiments to replicate the theoretical results and validate the modeling. To re-create the thickness in the modeling for the actual coating practice, we construct the thickness-concentration correlation for each polymer, as shown in **Figure S13**. Specifically, solutions with varying concentrations of the three polymers are prepared and spin-coated on glass/ITO substrates at the speed of 1500 rpm. The thicknesses of these films are measured using a profilometer or AFM and fitted as a function of the related concentrations for each polymer. Under the guidance of the

thickness-concentration correlations, polymer stackings with target thicknesses are coated. Measured transmittance spectra of the ECP stackings are shown by black curves in **Figure 2b**. Remarkably, they are in excellent agreement with modeling values (red dashed curves), providing the effectiveness of the modeling. Further, xyz chromaticity values are extracted from the experimental and simulated spectra (as shown in **Table S3**) and used to forecast the color appearances of the films. As shown in solid and dashed boxes, the colors from the experimental and modeling spectra are well matched.

Figure 2c shows the spectroelectrochemical performances of the three stacking electrochromic films. After oxidation and reduction cycles (electrochemical conditioning), the transmittance spectra exhibit some variations from the as-coated one, attributing to the morphological changes caused by ion penetration and extraction during electrochemical cycling. This suggests that the optical modeling value may have some disparity when predicting the color appearance of the film after cycling. However, the small deviation can be solved by using the optical constant values of films after electrochemical conditioning for optical modeling. The significant transmittance change between reduced (colored) and oxidized (bleached) states indicate that the stacking ECPs present promising electrochromic performances. The double potential step chronoabsorptometries and long cycling tests of the stacking ECPs are shown in **Figure S14** and their coloration efficiencies, optical contrasts, and cycling performances are summarized in **Table S4**. The maximum achievable optical contrasts of the ECP stackings are limited by the low-contrast components of the stacked polymers. For instance, when ECP-M is layered with ECP-Y, the optical contrast of the stacking is comparable to ECP-Y, which has a low optical contrast. For reference, spectroelectrochemistry of single-layer ECP-C, ECP-M, ECP-Y are shown in **Figure S15**.

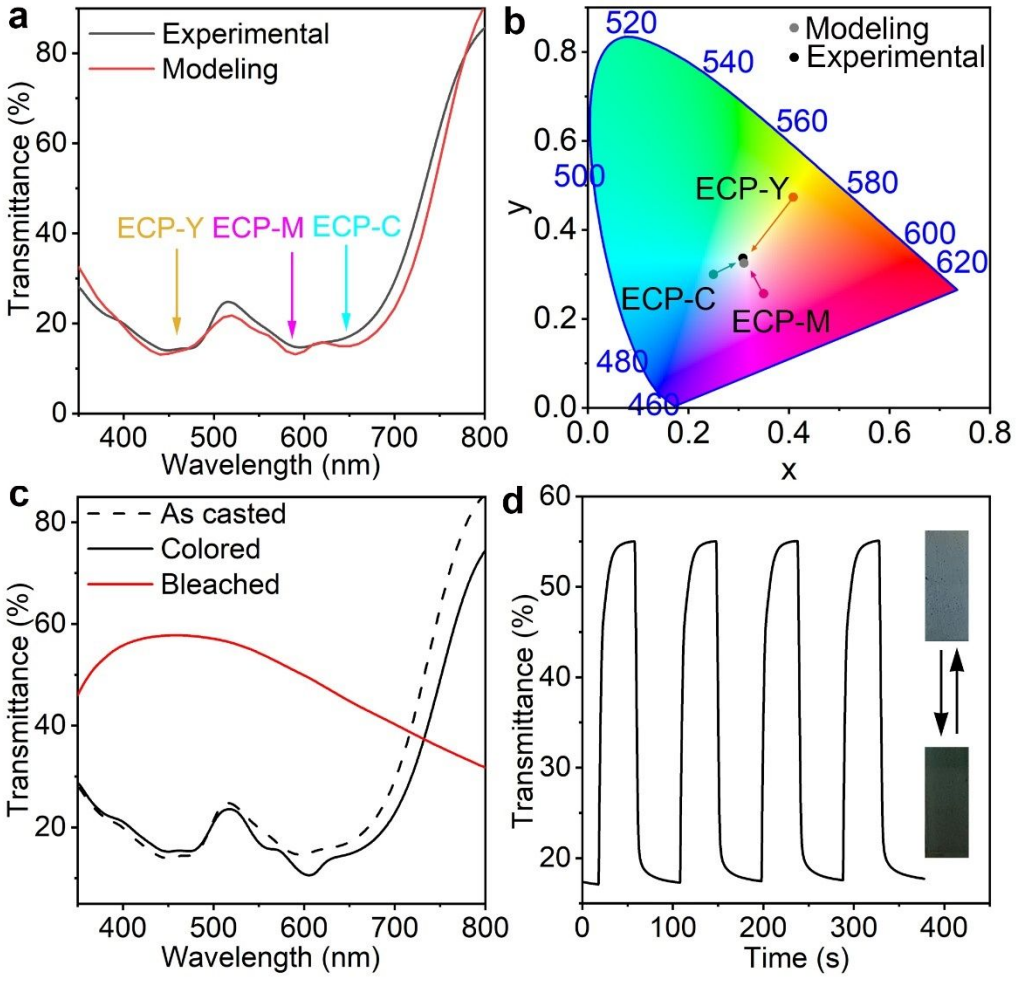

Fig. 3 Neutral grey electrochromic polymer from a triple-layer ECP. (a) Experimental vs. modeling spectra of the triple-layer ECP. (b) Chromaticity values extracted from the modeling and experimental spectra of the triple-layer ECP. The xy values of the constituent single-layer ECP-C, ECP-M, ECP-Y are also shown aside. (c) Spectroelectrochemistry and (d) double potential step chronoabsorptometry of the triple-layer ECP.

Next, we utilize the optical modeling to guide the preparation of a neutral grey ECP by stacking ECP-C, ECP-M, ECP-Y with appropriate thickness ratios. Neutral grey electrochromic materials have aroused great interest due to their wide applications.[26,27] According to the CMY color model, when cyan, magenta, and yellow electrochromic polymers (ECPs) are mixed with equal color contributions, their mixture will display neutral grey. However, since ECP-C, ECP-M, ECP-Y have distinct absorption coefficients, their mixing ratio must be carefully tuned to obtain neutral grey, which necessitates dedicated experimental labor. Through optical modeling, we predict when the film thicknesses of ECP-C, ECP-M, ECP-Y are 250 nm, 80 nm, and 100 nm respectively, the maximum absorbance intensities of the three polymers are almost identical, as shown in **Figure 3a**. In such a case, the stacking appears neutral grey. This is also supported by the fact that the xy chromaticity values extracted from modeling spectra are close to the coordinates of white point in color space, as shown in **Figure 3b**. Guided by the modeling and the concentration-thickness correlations, a triple-layer ECP stacking is prepared by depositing the three polymers in the sequence ECP-C/ECP-Y/ECP-M on the glass/ITO substrate from their chloroform solutions with concentrations of 26 mg/mL, 11 mg/mL, and 12 mg/mL, respectively. As shown in **Figure 3a** and **3b**, the experimentally obtained stacking electrochromic film exhibits almost identical transmittance as well as xy values as that of the modeling results. Further the spectroelectrochemistry, double potential step chronoabsorptometry, and pictures of the stacking polymer are shown in **Figure 3c** and **3d**. After electrochemical conditioning, a slight transmittance shift is observed, which attributes to the morphological change caused by ion penetration and extraction during the electrochemical cycling. The triple-layer electrochromic film shows 38% of optical contrast at 555 nm between colored and bleached states, with a switching time of 9 s, which is competitive among the reported neutral grey polymers.[26–32]

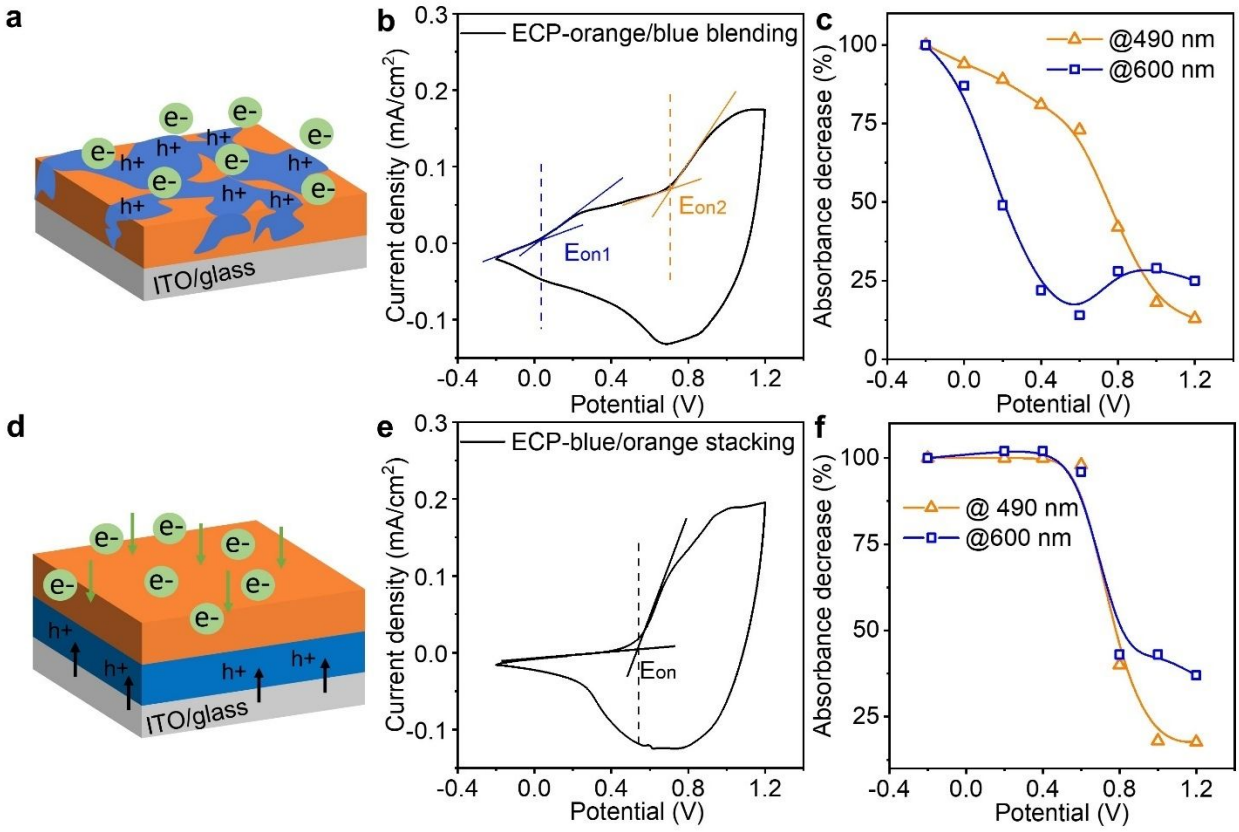

Fig. 4 Minimizing intermediate colors via unifying electrochemical onset potentials. Electrochemical doping illustrations, cyclic voltammograms, and absorbance decrease of (a-c) ECP-orange/blue blending and (d-f) ECP-orange/blue stacking.

After establishing the ECP stacking and modeling, we study the impact of stacking sequence on minimizing intermediate colors. Having intermediate color is a common issue in the reported co-processed electrochromic polymers (ECPs), due to the disparity of electrochemical onset potentials of constituent ECPs.[33,34] In our design, via controlling the stacking sequence of ECPs, their electrochemical onset potentials are synchronized to minimize the intermediate colors. Here, we employ two well-studied ECP-orange and ECP-blue to demonstrate this approach, since they have very distinct electrochemical onset potentials (0 V and 0.7 V *vs*. Ag/AgCl for ECP-blue and orange respectively).[35,36] The molecular structures of the polymers are shown in **Figure S16**. As a reference, we first study the electrochromic performance of their blends. As illustrated in **Figure 4a**, when the two polymers are blended and deposited on electrode, the ECP-blue with lower electrochemical onset potential will get oxidized first in response to an applied positive electric field, attracting anions from the electrolyte to enter the polymer film. As a result, the cyclic voltammetry of the film presents two separate electrochemical onset potentials at around 0 V and 0.7 V (**Figure 4b**), indicating a split electrochemical doping. To monitor the color change, we record their absorbance responses during the doping (**Figure S17**) and plot their absorbance decrease at the wavelength of 490 nm and 600 nm— which are around the maximum absorbance of ECP-blue and ECP-orange—as a function of applied voltage as shown in **Figure 4c**. At 0 V, the absorbance at 600 nm starts to decrease, while the absorbance at 490 nm does not exhibit a significant decrease until 0.6 V. This suggests that ECP-blue bleaches earlier than ECP orange. On the contrary, when the two polymers are stacked with ECP-orange on top, electrons will be extracted from ECP-blue to ITO while ions have to diffuse from ECP-orange/electrolyte interface to the whole ECP stacking under a positive potential. Only when the ECP-orange is doped, will the ions diffusion become unimpeded to complete the doping of the stacking, as illustrated in **Figure 4d**. In **Figure 4e**, this mechanism is proved by the CV of the ECP stacking, where a single electrochemical onset potential at around 0.58 V is observed, indicating a synchronized electrochemical reaction. **In Figure 4f**, the absorbance decreases at 600 nm and 490 nm are also in sync, suggesting a binary colored-to-bleached switching.

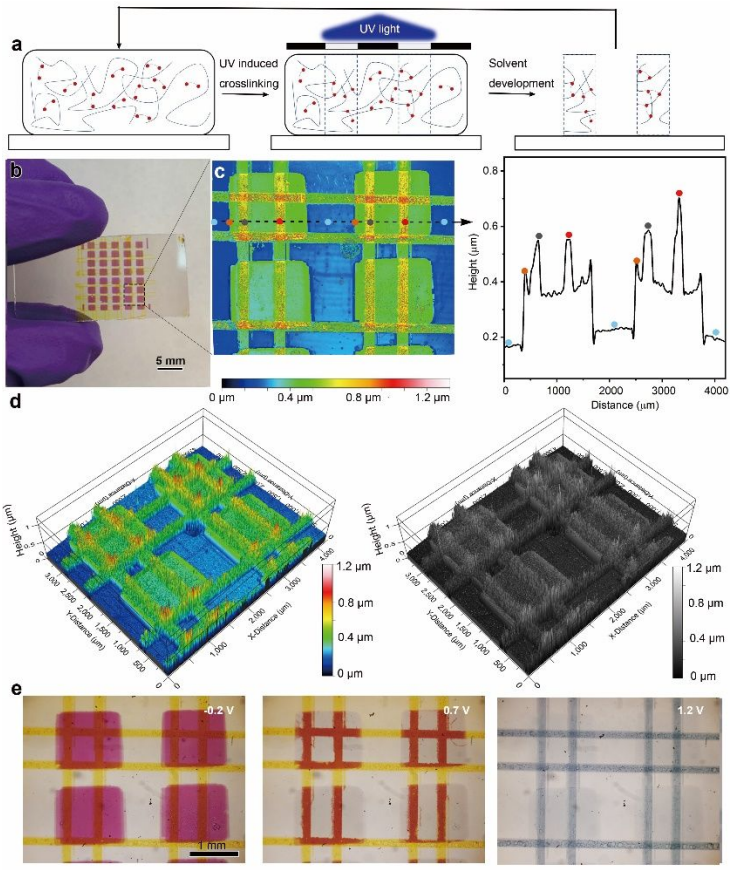

Fig. 5 Multilayer electrochromic patterns with layered textures. (a) Schema illustrating the photolithography printing of multilayer electrochromic patterns. (b) Digital picture of a multilayer electrochromic pattern. (c) 2D height map of the multilayer pattern with an extracted profile specifying the height change along the dashed line. (d) color-rendered and greyscale-rendered 3D topographies of the multilayer pattern. (e) Optical microscopic images showing the electrochromism of the pattern.

Lastly, taking advantage of the UV-triggered cross-linking and the solution-processable ECP stacking strategy, we use photolithography to create delicate patterns with layered textures. The printing process is illustrated in **Figure 5a**. Specifically, the multilayer ECP patterned are constructed with a series of repeated process including a photomask covering, 5 minutes of UV illumination and solvent development. The areas that are exposed to UV illumination are crosslinked while the remaining uncross-linked film is washed away using chloroform. The whole printing process is efficient, without use of any photoresists. As a demonstration, **Figure 5b** shows a multilayer ECP pattern consisting of magenta rectangles at the bottom and two pair of perpendicular yellow lines in the middle and at top layers. After obtaining the multilayer pattern, we use an optical profilometer to map out a representative periodic structure of this pattern as shown in **Figure 5c**, where the color codes indicate the height of the ECP surface. Remarkably, three height differences are observed on the substrate surface: green rectangular patterns (single layer), orange lines on rectangular patterns (double layer), and red intersections of the line patterns (triple layer). We further extract the height profile along the dashed line, from which the height changes at the junction of two features can be accurately obtained. Here, both the rectangular and line patterns have a thickness of around 200 nm. To visualize this height change in spatial dimensionality, the color-rendered and greyscale-rendered 3D surface topographies of the multilayer patterns are also displayed in **Figure 5d**, where various overhangs and undercut structures can be clearly observed. This reflects that rich texture information can be created based on the stacking strategy. Further, the electrochromism of the multilayer pattern is monitored under the optical microscope as shown in **Figure 5e**. At -0.2V, both the ECP-M and ECP-Y are in neutral states, making the rectangles and lines all in vivid color. At 1.2V, both lines and rectangular patterns are oxidized and thus bleached. While at 0.7 V, only ECP-M that is not covered by ECP-Y lines gets oxidized, since the insulating ECP-Y hinders the ion transmission and the oxidation of the bottom ECP-M. Thus, the lines on the top of ECP-M squares appear to be red. This observation matches the early discussion in Figure 4. The voltage-dependent ECP patterns enables a more informative color display.

Conclusion

In summary, we demonstrated a facile method to stack solution-processable electrochromic polymers (ECPs), which was achieved by co-processing ECPs with a crosslinker (bisFA). Triggered by UV light, the crosslinker endowed the ECPs with solvent-resistant properties without compromising their electrochromic performances and allowed them to be sequentially deposited. Following CMY subtractive color mixing theory, three primary ECPs (ECP-C, ECP-M, ECP-Y) were chosen to be stacked with a variety of thicknesses, generating a full-color palette. A COMSOL optical modeling was applied to guide the preparation of double-layer and triple-layer ECPs, producing targeted secondary and tertiary colors. We further integrated the stacking strategy with photolithography, constructing a multilayer ultraprecise ECP pattern with overhang and undercut textures, that displayed voltage-dependent electrochromic features. By placing the ECP with high electrochemical potential on top, the ECP stacking presented synchronized electrochemical potentials and almost binary colored-to-bleached switching with minimum intermediate colors. We believe this ECP stacking method will open an avenue for delicate ECP printing and display. Despite the benefits of the ECP stacking, its several aspects need to be further studied to carry this strategy forward. First, when the stacking is fully bleached, the components with lower potential windows may bear an overoxidation. Second, for a desired color, the thickness ratio of the stacked ECP films is fixed, which lessens the opportunity to adjust the film thickness of each layer for an optimal optical contrast.

Author Contributions

K.C. and J.M. conceived the idea and designed the experiments. K.C. performed the experiments, characterizations, and optical modeling. Y.W. prepared the crosslinker. L.Y. and W.W. prepared the electrochromic polymers. X.W. and K.Z. conducted the optical profilometer measurements. D.Z. and H.W. measured the thicknesses of ECP thin films and helped with optical modeling. J.E performed Filmetrics measurements. M.A. conducted DSC measurements. K.C. and J.M. drafted the manuscript, and all authors contributed to manuscript preparation.

Acknowledgements

We are grateful for the financial support from Ambilight Inc under contract #40001872. We thank Professor Yung C. Shin for providing the access to optical profilometer.

Conflicts of interest

J.M. is a co-founder of Ambilight Inc. A patent disclosure was filed.

Notes and references

1 T. Xu, E. C. Walter, A. Agrawal, C. Bohn, J. Velmurugan, W. Zhu, H. J. Lezec and A. A. Talin, Nat. Commun., 2016, **7**, 10479.
2 S. I. Cho, W. J. Kwon, S.-J. Choi, P. Kim, S.-A. Park, J. Kim, S. J. Son, R. Xiao, S.-H. Kim and S. B. Lee, *Adv. Mater.*, 2005, **17**, 171–175.
3 P. Andersson, R. Forchheimer, P. Tehrani and M. Berggren, *Adv. Funct. Mater.*, 2007, **17**, 3074–3082.
4 S. Chen, S. Rossi, R. Shanker, G. Cincotti, S. Gamage, P. Kühne, V. Stanishev, I. Engquist, M. Berggren, J. Edberg, V. Darakchieva and M. P. Jonsson, *Adv. Mater.*, 2021, **33**, 2102451.
5 Y. Kim, M. Han, J. Kim and E. Kim, *Energy Environ. Sci.*, 2018, **11**, 2124–2133.
6 J. Kim, M. Rémond, D. Kim, H. Jang and E. Kim, *Adv. Mater. Technol.*, 2020, **5**, 1900890.
7 C. Ma, M. Taya and C. Xu, *Polym. Eng. Sci.*, 2008, **48**, 2224–2228.

8 Y. Kondo, H. Tanabe, H. Kudo, K. Nakano and T. Otake, *Materials*, 2011, **4**, 2171–2182.
9 P. M. Beaujuge and J. R. Reynolds, *Chem. Rev.*, 2010, **110**, 268–320.
10 C. M. Amb, A. L. Dyer and J. R. Reynolds, *Chem. Mater.*, 2011, **23**, 397–415.
11 G. Sonmez, *Chem. Commun.*, 2005, **42**, 5251.
12 R. H. Bulloch, J. A. Kerszulis, A. L. Dyer and J. R. Reynolds, *ACS Appl. Mater. Interfaces*, 2014, **6**, 6623–6630.
13 A. M. Österholm, D. E. Shen, J. A. Kerszulis, R. H. Bulloch, M. Kuepfert, A. L. Dyer and J. R. Reynolds, *ACS Appl. Mater. Interfaces*, 2015, **7**, 1413–1421.
14 R. H. Bulloch, J. A. Kerszulis, A. L. Dyer and J. R. Reynolds, *ACS Appl. Mater. Interfaces*, 2015, **7**, 1406–1412.
15 J. D. Lieber and S. J. Bensmaia, *Proc Natl Acad Sci USA*, 2019, **116**, 3268–3277.
16 M. Holliins, R. Faldowski, S. Rao and F. Young, *Perception & Psychophysics*, 1993, **54**, 697–705.
17 S. Yan, H. Fu, L. Zhang, Y. Dong, W. Li, M. Ouyang and C. Zhang, *Chemical Engineering Journal*, 2021, **406**, 126819.
18 R.-Q. Png, P.-J. Chia, J.-C. Tang, B. Liu, S. Sivaramakrishnan, M. Zhou, S.-H. Khong, H. S. O. Chan, J. H. Burroughes, L.-L. Chua, R. H. Friend and P. K. H. Ho, Nat. Mater., 2010, **9**, 152–158.
19 L. A. Estrada, J. J. Deininger, G. D. Kamenov and J. R. Reynolds, *ACS Macro Lett.*, 2013, **2**, 869–873.
20 J. A. Kerszulis, C. M. Amb, A. L. Dyer and J. R. Reynolds, *Macromolecules*, 2014, **47**, 5462–5469.
21 C. M. Amb, J. A. Kerszulis, E. J. Thompson, A. L. Dyer and J. R. Reynolds, *Polym. Chem.*, 2011, **2**, 812.
22 B. D. Reeves, C. R. G. Grenier, A. A. Argun, A. Cirpan, T. D. McCarley and J. R. Reynolds, *Macromolecules*, 2004, **37**, 7559–7569.
23 P. M. Beaujuge, S. V. Vasilyeva, S. Ellinger, T. D. McCarley and J. R. Reynolds, *Macromolecules*, 2009, **42**, 3694–3706.
24 M. Schock and S. Bräse, *Molecules*, 2020, **25**, 1009.
25 C.-Y. Chang, B.-C. Tsai, Y.-C. Hsiao, M.-Z. Lin and H.-F. Meng, *Nano Energy*, 2019, **55**, 354–367.
26 S. V. Vasilyeva, P. M. Beaujuge, S. Wang, J. E. Babiarz, V. W. Ballarotto and J. R. Reynolds, *ACS Appl. Mater. Interfaces*, 2011, **3**, 1022–1032.
27 G. Öktem, A. Balan, D. Baran and L. Toppare, *Chem. Commun.*, 2011, **47**, 3933.
28 C. Wang, M. Wang, Y. Zhang, J. Zhao and C. Fu, *RSC Adv.*, 2016, **6**, 80002–80010.
29 M. İçli, M. Pamuk, F. Algı, A. M. Önal and A. Cihaner, *Organic Electronics*, 2010, **11**, 1255–1260.
30 M. Guzel, E. Karataş and M. Ak, *Smart Mater. Struct.*, 2019, **28**, 025013.
31 Z. Xu, H. Yue, B. Wang, J. Zhao, M. Wang, Y. Zhang and Y. Xie, *Materials & Design*, 2020, **194**, 108903.
32 K.-R. Lee and G. A. Sotzing, *Chem. Commun.*, 2013, **49**, 5192.
33 L. R. Savagian, A. M. Österholm, D. E. Shen, D. T. Christiansen, M. Kuepfert and J. R. Reynolds, *Advanced Optical Materials*, 2018, **6**, 1800594.
34 T. Jarosz, K. Gebka, A. Stolarczyk and W. Domagala, *Polymers*, 2019, **11**, 273.
35 K. Cao, D. E. Shen, A. M. Österholm, J. A. Kerszulis and J. R. Reynolds, *Macromolecules*, 2016, **49**, 8498–8507.
36 J. F. Ponder, A. M. Österholm and J. R. Reynolds, *Macromolecules*, 2016, **49**, 2106–2111.